agriculture

MDPI

Article

Design and Testing of a Whole-Row Top-Loosening Stem-Clamping Seedling Extraction Device for Hole Tray Seedlings

Zehui Peng [1], Fazhan Yang [1,*], Yuhuan Li [1], Xiang Li [1], Baogang Li [1,2] and Guoli Xu [1]

[1] School of Mechanical and Automotive Engineering, Qingdao University of Technology, Qingdao 266520, China; 15624498910@163.com (Z.P.); 19560870296@163.com (G.X.)
[2] State Key Laboratory of Mechanical Transmission, Chongqing University, Chongqing 400044, China
* Correspondence: fazhany@163.com

Abstract: A combined seedling extraction device was developed that operates by first top loosening and then clamping the stem in order to solve the current issues with automated transplanting technology, such as low seedling extraction efficiency and a high rate of substrate loss. The pepper plug tray seedlings were selected as the experimental subjects for testing the mechanical properties of the stems. The tensile and compressive mechanical properties of the stems were obtained, and the kinematic model of the seedling spacing process and the mechanical model of the seedling clamping process were established. Key parameters of the seedling extraction device were analyzed and calculated, and an automated seedling extraction system was constructed. Using substrate moisture content, seedling age, and extraction frequency as experimental factors, orthogonal tests were conducted. Through variance analysis and 3D response surface analysis, the optimal rounded parameter values were determined: 48% substrate moisture content, 38-day-old seedlings, and a seedling extraction frequency of 60 plants/min. Under these conditions, the seedling extraction success rate was 94.44%, the substrate loss rate was 6.07%, and the seedling damage rate was 4.17%, meeting the requirements for automated seedling extraction.

Keywords: agricultural machinery; transplanter; hole tray seedling; seedling-picking mechanism

check for updates

Academic Editor: Ju-Seok Nam

Received: 9 December 2024
Revised: 1 January 2025
Accepted: 11 January 2025
Published: 13 January 2025

Citation: Peng, Z.; Yang, F.; Li, Y.; Li, X.; Li, B.; Xu, G. Design and Testing of a Whole-Row Top-Loosening Stem-Clamping Seedling Extraction Device for Hole Tray Seedlings. *Agriculture* **2025**, *15*, 165. https://doi.org/10.3390/agriculture15020165

Copyright: © 2025 by the authors. Licensee MDPI, Basel, Switzerland. This article is an open access article distributed under the terms and conditions of the Creative Commons Attribution (CC BY) license (https://creativecommons.org/licenses/by/4.0/).

1. Introduction

Vegetable seedling transplanting technology, when compared to direct seeding, offers several advantages, including shortened growth cycles, improved land utilization, and enhanced resistance to cold and pests, which have led to its widespread adoption [1–3]. Currently, manual and semi-automated transplanting methods dominate in the PRC, though these practices are plagued by issues such as low seedling extraction efficiency, high labor intensity, and substantial time costs [4–7]. As agriculture advances toward greater intelligence and precision, traditional mechanized technologies fall short of modern production demands. Automated seedling-picking technology, by replacing manual operations with mechanized precision, can dramatically improve efficiency and accuracy. Thus, developing automated seedling-picking systems is crucial for advancing fully automated transplanting machines [8]. As a critical component of fully automated transplanting systems, the quality of seedling extraction directly impacts the overall performance of the transplanting operation [9]. Therefore, the development of a seedling extraction mechanism characterized by low seedling damage, high extraction efficiency, and minimal substrate loss is of the utmost significance for improving the quality of vegetable tray seedling transplanting and advancing research on automated transplanting equipment [10–12].

The seedling extraction mechanism is the core component of fully automated transplanting machines, and it has been the subject of extensive research by numerous scholars both domestically and internationally [13–15]. Khadatkar et al. [16] designed a robotic plug-in seedling extraction mechanism, which integrates sensor-based positioning technology. This system achieves high extraction quality, with a seedling loss rate as low as 7.6%. However, the mechanism is complex and costly. Liu et al. [17] designed a stem-gripping seedling extraction device based on machine vision, tailored to the characteristics of tomato plug seedlings. The system employs the YOLOv5 algorithm to precisely control the extraction claws, enabling intelligent seedling extraction. The device achieves a damage rate of 7.2% and a seedling extraction success rate exceeding 90.3%. Zhou et al. [18] designed a pepper seedling extraction mechanism utilizing an eagle beak probe, which incorporates a crank mechanism converted into a non-circular gear planetary drive to meet the posture requirements of plug seedlings. With a single rotation, the device grasps two seedlings, improving production efficiency and achieving a maximum success rate of 96.4%. However, its structure is relatively complex, and its precision is suboptimal. Rahul et al. [19] developed a two-degree-of-freedom parallel-link seedling extraction device with five rotating joints. The device employs a dual-claw gripper mounted at the joints of two linkages. This design features a simple structure and a high degree of automation, but it suffers from low extraction efficiency and is not suitable for high-speed transplanting. Zhou et al. [20] also designed a pneumatic-mechanical hybrid seedling extraction device, featuring a reduced pin height and a gripping mechanism, which minimizes substrate loss. The overall seedling extraction success rate of this system is 91.69%. Hu et al. [21] proposed an automatic seedling extraction device based on a clamping rod. By establishing a double-crank linkage motion model, they optimized the trajectory to achieve a high seedling extraction success rate of over 91.1%. However, the device operates at a relatively low extraction frequency.

In summary, current automated seedling extraction devices exhibit relatively complex structures and are prone to issues such as seedling clipping failure and substrate block damage during the extraction process. This paper presents the design of a row-based top-loosening and stem-gripping combined seedling extraction device, which employs pneumatic ejection and stem gripping for seedling extraction. This approach effectively addresses problems such as high substrate loss and low extraction success rates. Using pepper seedlings as the test subject, the study measures key physical parameters of the plug seedlings, establishes mechanical and kinematic models, and analyzes the seedling clipping and ejection processes. Key parameters are identified, and based on the row-based seedling extraction and evenly spaced seedling ejection methods, an automatic seedling extraction system is developed. An orthogonal experiment is conducted to optimize operational parameters, thereby verifying the success rate and stability of the device. The results provide a valuable reference for the development and design of fully automated transplanting machinery.

2. Materials and Methods

2.1. Mechanical Properties of Hole Tray Seedlings

The row-based top-loosening and stem-gripping operation involves actions such as ejection, gripping, and extraction of the plug seedlings. In this study, 20 pepper seedlings, aged between 30 and 45 days, were randomly selected as the test subjects. The growing medium consisted of a mixture of vermiculite, perlite, and peat moss in a 1:1:2 ratio. All experiments were conducted at room temperature. The morphological parameters and positions of the seedlings were calibrated as shown in Figure 1, with the results summarized in Table 1. The mechanical properties were tested and analyzed using the TA.XT Plus texture

analyzer, with the aim of providing data support for the structural design and parameter optimization of the top-loosening and stem-gripping seedling extraction device.

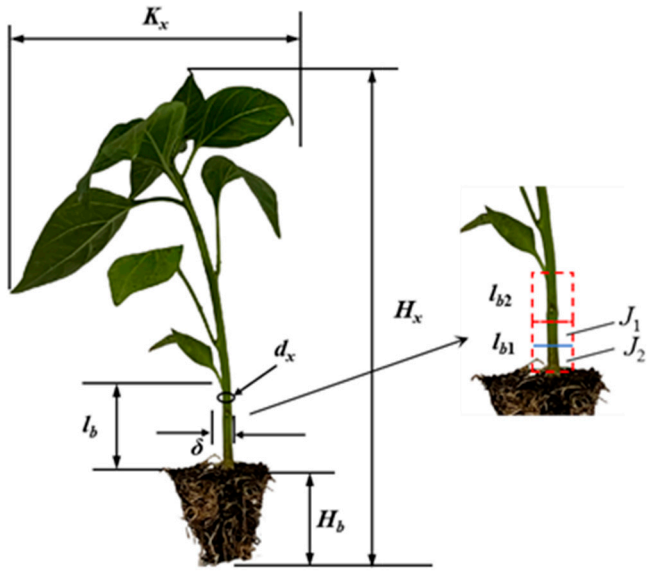


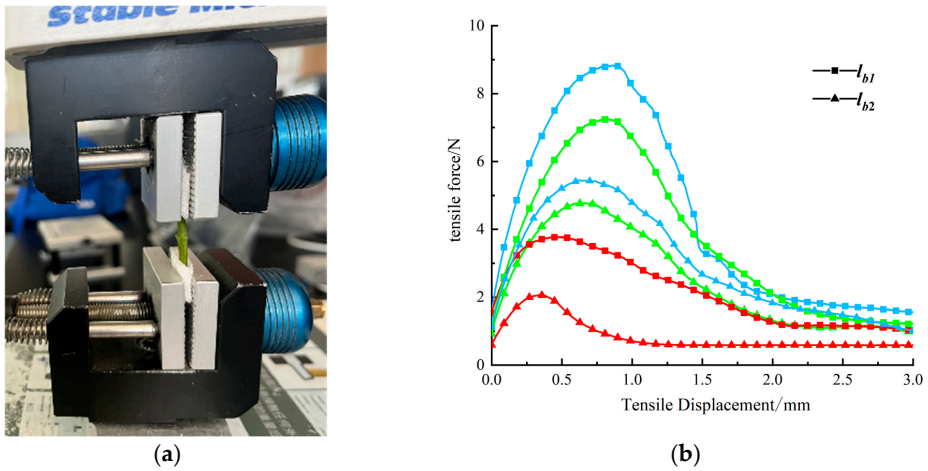
Figure 1. Morphology of burrowed seedlings. K_x—width of the leaf surface; H_x —total height of the hole tray seedling; H_b—height of the mantle; d_x—diameter of the stalk; l_b—distance from the mantle to the first leaf blade; δ—offset of the stalk from the centerline; l_{bi}—segmentation from the bottom of the mantle to the first leaf blade.

Table 1. Morphological parameters of burrowed seedlings.

Morphological Parameters	Numerical Value	Average Value
Total height of hole tray seedlings H_x/(mm)	129~163	141
Leaf surface width k_x/(mm)	93~148	122.63
Stem diameter d_x/(mm)	2.82~3.44	3.21
Distance from mantle to first blade l_{bi}/(mm)	29~52	42.12
Stem offset from centerline δ/(mm)	2.1~12.6	8.13
Mantle height H_b/(mm)	32.4~37.5	35.05
Individual hole tray seedling mass m/(g)	9.3~16.2	12.5

2.1.1. Stem Tensile Characterization Test

To accurately locate the gripping and extraction positions, the seedling stem was divided into two segments based on the dimensions from the plug body to the first leaf. These segments were designated as l_{b1} (0–20 mm) and l_{b2} (20–40 mm). The tensile testing process is illustrated in Figure 2a. During the test, the seedling stem was secured using a tensile fixture and mounted on the test bench, maintaining a vertical alignment relative to the horizontal plane. To prevent damage or slippage of the seedling stem during stretching, which could affect the results, the gripping positions were wrapped with gauze. In the experiment, the lower gripping point was located near the plug body end, while the upper gripping point was positioned at the top of the stem. The initial loading process was carried out at a constant speed of 1 mm/s, with a stretching displacement of 5 mm.



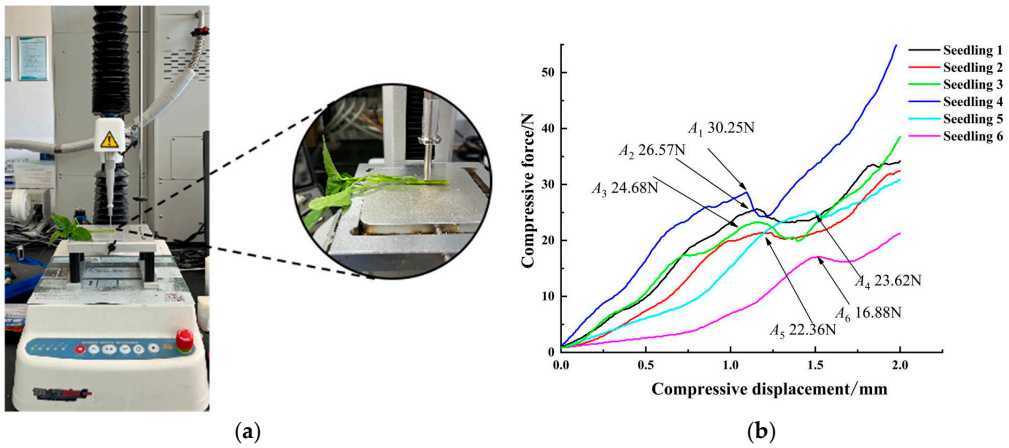
(**a**) (**b**)

Figure 2. Stem tensile test. (**a**). Tensile test effect diagram; (**b**). Tensile force vs. displacement curves (The curves of the same color are the variation curves of different weighting positions of a potting seedling).

From the tensile force versus displacement curve shown in Figure 2b, it can be observed that the curve is divided into three distinct segments. The first segment shows a steady increase in the tensile strength of the stem as the displacement increases, reaching the breaking point. In the second segment, after reaching the breaking force, the tensile force begins to decrease as the displacement continues, eventually approaching zero. The third segment shows the post-fracture behavior, where the stem exhibits significant non-elastic characteristics; the tensile force is no longer proportional to further displacement, and it no longer increases with displacement. Within the same seedling, the gripping position significantly affects the tensile strength of the seedling stem. The tensile strength in the l_{b1} segment is greater than in the l_{b2} segment, indicating that higher gripping positions result in a decrease in tensile strength. This is because the lb1 segment, which is closely connected to the plug body, has higher strength due to its abundant nutrients and thicker fibers. However, as the gripping position rises, the stem diameter gradually decreases, leading to a reduction in tensile strength. Considering these factors, the l_{b1} segment is selected as the optimal extraction region. Furthermore, the l_{b1} segment is divided into two parts, J_1 and J_2, from the root to the top, each with a length of 10 mm. However, to avoid interference between the gripping mechanism and the plug body, the optimal gripping region is determined to be the J_1 segment (10–20 mm).

2.1.2. Stem Compression Characterization Test

To accurately assess the appropriate gripping force required for the seedling extraction mechanism and to avoid damaging the seedling stem due to excessive compression, it is necessary to investigate the compressive characteristics of the stem. As determined in Section 2.1.1, the testing point is located at the base of the pepper seedling stem, specifically in the l_{b1} segment (0–20 mm) from the root end. The compression test is shown in Figure 3a. First, the sample was placed flat between a metal plate and the probe, with the angle precisely adjusted to ensure that the stem was directly beneath the probe, ensuring tight contact and uniform force distribution. In the experiment, the compression ratio was set to 60%, meaning that during the downward motion of the probe, the compressed length of the stem was 60% of its diameter. The loading speed was set at 10 mm/min, a rate that both prevents damage to the stem and allows for accurate data collection.



(**a**) (**b**)

Figure 3. Stem compression characteristic test. (**a**). Compression test chart; (**b**). Compression force versus displacement plot.

As shown in Figure 3b, the deformation curve of the stem's compressive characteristics is similar and can be divided into two stages. The OA segment represents the elastic phase, where the compressive load increases linearly with the compression displacement. During this phase, the compressive force has little effect on the stem, and once the load is removed, the stem can self-recover. The point A is referred to as the biological yield point. After point A, the second phase begins, where the compressive load continues to increase, leading to the rupture of the epidermal cells of the stem, damaging its structure. As a result, the stem cannot return to its normal state, affecting subsequent growth and development and compromising transplant quality. The measured average yield force at point A is 24.06 N. When designing the gripping mechanism, the gripping force must be kept below this critical value, ensuring that the stem's integrity is maintained and transplant success is achieved.

2.2. Structure and Working Principle of the Whole Machine

2.2.1. Structure of the Whole Machine

This study focuses on the 72-cell (6 × 12) vegetable seedling tray, and the developed automatic seedling extraction device employs a combined mechanical, electrical, and pneumatic system to perform actions such as automatic tray feeding, seedling lifting, seedling gripping, seedling spacing, and seedling placement. The device, as shown in Figure 4, consists of a frame, tray conveyor, seedling lifting mechanism, seedling extraction mechanism, compression plate mechanism, and control system. The seedling extraction mechanism is composed of a seedling end effector (parallel pneumatic claws), a lifting pneumatic cylinder, a sliding pneumatic cylinder, and a scissor mechanism. The goal of the seedling extraction mechanism is to remove each seedling from the tray one by one. Through precise trajectory control, it ensures that each seedling is accurately placed into a designated seedling cup, thus simplifying the extraction process and improving transplant efficiency. The overall control strategy of the seedling extraction mechanism follows the sequence of seedling extraction—seedling spacing—seedling placement. After the seedlings are ejected from the tray, they are gripped by the end effector, and the seedling spacing is controlled by the scissor mechanism, which is operated by the spacing pneumatic cylinder, thereby completing a single extraction cycle.

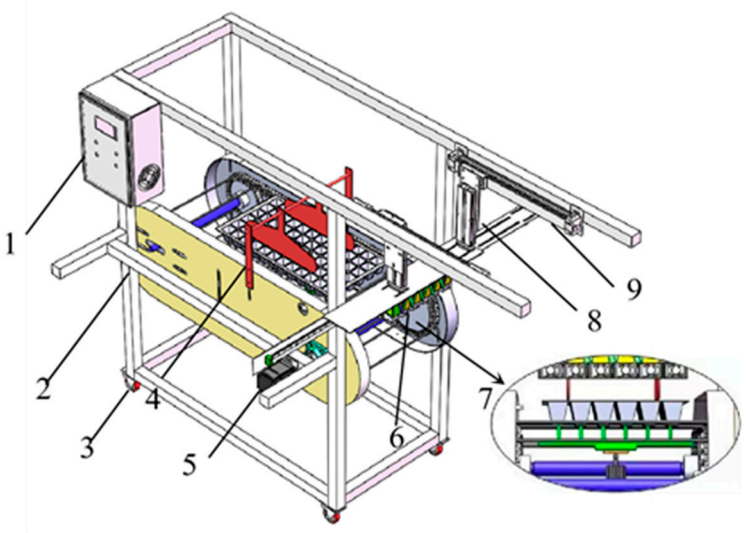


Figure 4. Complete machine diagram of the seedling extraction device. 1. Control box; 2. Frame; 3. Casters; 4. Platen mechanism; 5. Motor; 6. Seedling dividing mechanism; 7. Top seedling mechanism; 8. Lifting mechanism; 9. Shifting mechanism.

2.2.2. Working Principle

The operation process of the seedling extraction mechanism and the movement of the seedlings are illustrated in Figure 5. The seedling trays are uniformly placed on the tray conveyor. During operation, a push rod serves to support and position the trays. Under the rotation of the stepper motor, the tray moves to the predetermined seedling extraction position. When the stepper motor stops, the seedling extraction process begins with the assistance of the seedling lifting and gripping mechanism. The extraction process consists of five stages:

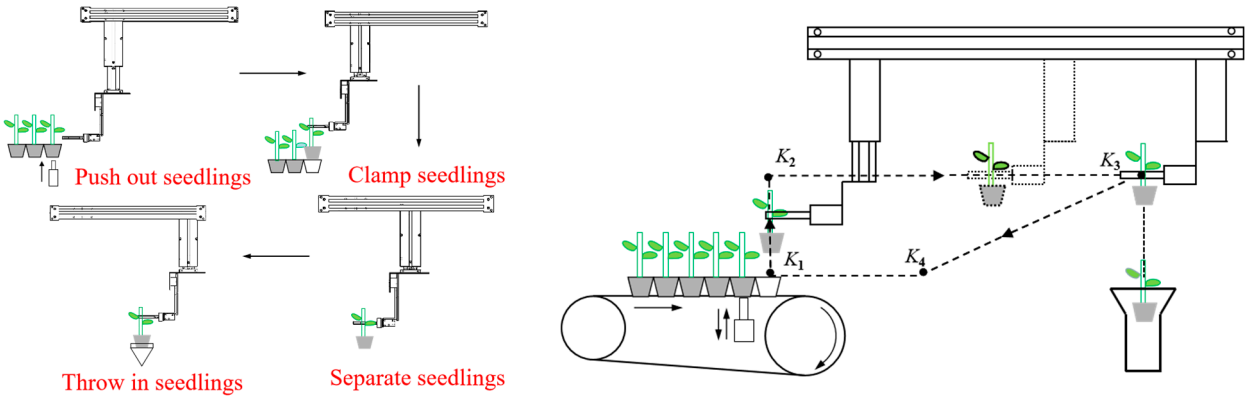


Figure 5. Schematic diagram of seedling taking mechanism. (**a**). Flow chart of seedling extraction process (The direction of the arrow represents the movement step of the seedling extraction process); (**b**). Potting position transformation diagrams (The direction of the arrow represents the trajectory path of the end-effector of the seedling picker).

(1) Seedling Lifting: After the tray is accurately positioned, the drainage holes align with the push rod. The position sensor detects the tray and sends a signal to the lifting cylinder, which extends and ejects the seedlings by a specified displacement;
(2) Seedling Gripping: The lifting pneumatic cylinder descends to the gripping position (point K_1), aligning with the seedling tray. The end effector of the seedling extraction mechanism closes, gripping the seedling's stem;

(3) Seedling Extraction: Once the seedling is gripped, the lifting pneumatic cylinder ascends, pulling the seedling out of the tray. The movement follows the trajectory from K_1 to K_2;
(4) Seedling Spacing: The sliding pneumatic cylinder moves horizontally, and the spacing mechanism extends to distribute the seedlings above the corresponding seedling cups. The movement follows the trajectory from K_2 to K_3;
(5) Seedling Placement: The end effector opens, and the seedling falls under gravity into the seedling cup, completing the extraction process. Subsequently, all cylinders return to their original positions. During this process, the stepper motor operates to move the seedling tray forward to the sensor's position. The end effector then returns to point K_1, and the movement follows the trajectory from K_3 to K_4 and back to K_1. This cycle repeats to complete the automated seedling extraction.

2.3. Key Component Design and Optimization Analysis

2.3.1. Design of the Shear Mechanism

To enhance the accuracy and stability of the seedling spacing process in the full-automatic seedling extraction mechanism with the row lifting and stem gripping method, a cost-effective, simple, and stable scissor-type spacing mechanism is designed to ensure the even and consistent spacing of the seedlings by the end effector. The mechanism, as shown in Figure 6, consists of parallel components including a guide rail, sliding blocks, seedling spacing plates, and scissor plates, which are fixed together by bolts. The two ends of the scissor plates are connected with hinge pins to allow for horizontal extension during the seedling spacing process. The guide rail of the seedling spacing mechanism is equipped with six sliding blocks, each of which is connected to a seedling spacing plate. One end of the mechanism is fixed by a stopper block to secure the sliding blocks, while the other end is designed to be movable. The seedling spacing cylinder is bolted to the sixth sliding block, providing the input power to drive the mechanism's back-and-forth motion. During seedling extraction, the scissor mechanism is in a contracted state, aligning with the seedling cells of the tray. During the spacing process, the mechanism expands and disperses, corresponding to the seedling cups on the conveyor chain.

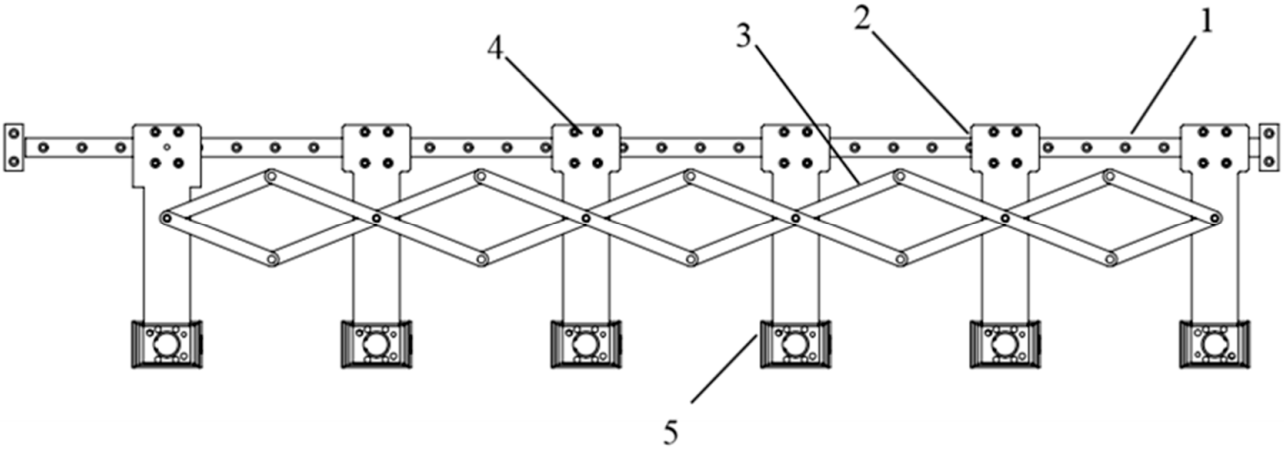


Figure 6. Three-dimensional model of shear mechanism. 1. Guide rail; 2. Slider; 3. Shear plate; 4. Seedling dividing plate; 5. Clamp seedling end actuator.

Motion Analysis of the Shear Mechanism

The scissor-type seedling spacing mechanism offers numerous advantages, such as low cost and simple structure. A thrust F_w is applied to the free end of the spacing mechanism to enable forward sliding and equal-distance dispersion. On the flexible seedling conveyor

chain, the distance C between two adjacent seedling cups is 118 mm, while the distance B between two seedling cells in a standard 72-cell tray is 43 mm. The width of the sliding block should be smaller than the distance B, and the width of the seedling spacing plate should be the same as the gap between adjacent sliding blocks when closed, which is also 43 mm. This ensures that the seedling cups align properly and facilitates the accurate gripping of the seedling stems. A rectangular coordinate system is established with the origin at the fixed end. The direction of seedling spacing is taken as the x-axis, and the vertical direction is taken as the y-axis, as shown in Figure 7. Based on this, the equations are derived as follows:

$$\begin{cases} C = l_2 \\ B = l_1 \\ H = l_2 - l_1 = 2R(\cos\theta_2 - \cos\theta_1) \\ X_1 = n2Rcos\theta_1 \\ X_2 = n2Rcos\theta_2 \end{cases} \quad (1)$$

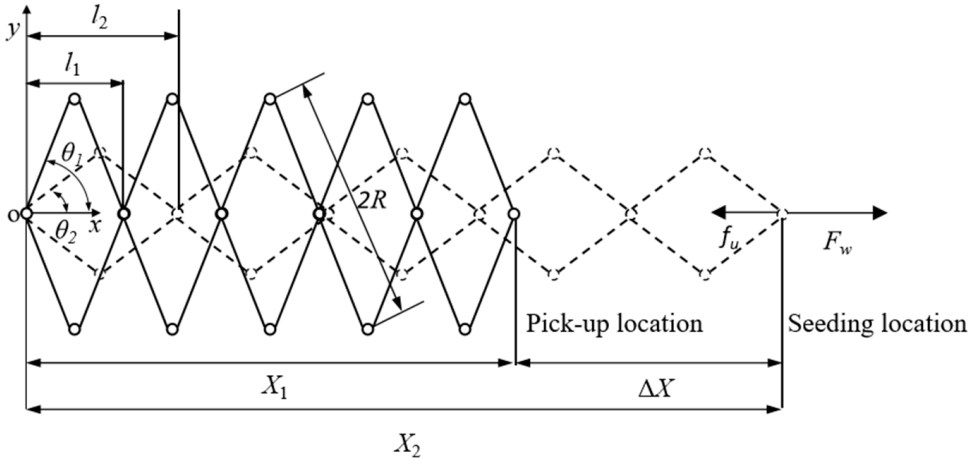


Figure 7. Sketch of the motion of the shear mechanism.

In the formula, l_1—distance between adjacent sliders when the shear mechanism is closed; l_2—distance between adjacent sliders when the shear mechanism is dispersed; 2R—length of the shear bar arm of the shear mechanism; θ_1—the angle between the centerline of the shear-rod arm and the vertical direction of the straight plate when it is closed; θ_2—the angle between the centerline of the shear-rod arm and the vertical direction of the straight plate when it is dispersed; X_1—distance from the seedling plate to the fixed end when closing; X_2—distance from the seedling plate to the fixed plate when dispersing, mm; ΔX—stroke distance of the seedling-splitting cylinder's expansion and contraction.

This gives the shear bar arm length, as follows:

$$2R = \frac{H}{\cos\theta_2 - \cos\theta_1} \quad (2)$$

Cylinder stroke:

$$\Delta X = X_2 - X_1 = n2R(\cos\theta_2 - \cos\theta_1) = n2R\cos\Delta\theta \quad (3)$$

In general, θ_1 should not exceed 80° to prevent excessive force increase when the shear fork mechanism's cylinder retracts, as larger θ_1 angles lead to higher thrusts. Meanwhile, θ_2 must remain within a reasonable range [22]: if θ_2 is less than 35°, decreasing the an-

gle has little impact on the stroke of the shear, and could lead to instability; conversely, if θ_2 exceeds 50°, the full potential of the shear arm cannot be utilized. Setting θ_1 to 76° and θ_2 to 41°, along with dimensions such as l_1 = 43 mm and l_2 = 118 mm, when these values are incorporated into Equations (2) and (3), the rounded results yield 2R = 146 mm and the dimension change, ΔX, amounts to 447 mm.

When the seedling separation cylinder extends, due to the very short acceleration time, it can be considered as uniform acceleration motion. The acceleration and deceleration of the seedling during the separation process significantly affect the substrate of the seedling. Therefore, it is necessary to reduce the acceleration of the slider. In the case of the seedling-taking frequency of 90 plants/min, a seedling-taking cycle takes 4 s, and the seedling-splitting cylinder running time is t_1 = 0.8 s.

$$\begin{cases} v_1 = \frac{\Delta X}{t_1} \\ a_1 = \frac{v_1}{t_2} \end{cases} \tag{4}$$

In the formula, v_1—the maximum speed of the cylinder when it extends, m/s; t_1—the time of cylinder movement, s; a_1—the acceleration of the cylinder on the slider, m/s^2; t_2—the time of the cylinder in the acceleration phase, s.

Assuming that the sliders are rigidly connected to each other and ignoring the tension between each shear plate, they are subjected to equal friction, which is obtained according to Newton's second law, as follows:

$$\begin{cases} F_w - 5f_u = 5m_w a_1 \\ f_u = \mu_1 m_w g \end{cases} \tag{5}$$

In the formula, F_w—the tension of the seedling-splitting cylinder, N; f_u—the friction between the single slider and the guide rail, N; m_w—the total mass of the seedling-taking end-effector, kg.

During the extension of the seedling spacing cylinder, the acceleration phase, controlled by the solenoid valve, is very short, followed by uniform motion. If the acceleration during the spacing process is too high, the movement becomes jerky, causing noticeable shaking of the machinery, which in turn leads to damage to the substrate blocks. Therefore, it is necessary to reduce the acceleration of the sliding block. The acceleration time t_2 is set to 0.1 s, and the total mass of the end effector, m_w, is 0.5 kg (including the seedling gripping cylinder, gripping plate, and seedling spacing plate). The friction between the sliding block and the guide rail is assumed to be rolling friction, with a coefficient of friction μ_1 set to 0.15. Substituting into the Formula (5), the minimum pull force of the seedling-splitting cylinder is 17.72 N. The cylinder stroke must be greater than the reciprocating stroke ΔX of the scissor mechanism. We selected the MAL20-450 pen-type cylinder as the seedling spacing cylinder, which meets the design requirements according to the relevant manual.

2.3.2. Seedling Clamping Device

Seedling Clamping Device Design

The seedling gripping mechanism adopts a pneumatic system, which offers advantages such as fast response, precision, and stability. It consists of parallel finger cylinders and gripping plates. By controlling the opening and closing of the solenoid valve, the parallel finger cylinders are activated to drive the gripping plates for opening and closing, allowing for the grasping and placement of seedlings in the tray. This mechanism plays a crucial role in enabling the automation of seedling extraction and placement.

To ensure accurate gripping of the seedling stems, the following design requirements must be considered: (1) when the gripping claws are open, the interference between

adjacent claws must be avoided to ensure smooth operation; (2) during the gripping process, the angle of the claws must be carefully controlled to accommodate seedlings that may deviate from the center of the tray, preventing gripping failure; and (3) during closure, the gripping force should be moderate, avoiding excessive pressure that could damage the seedling stems. The structural parameters are shown in Figure 8.

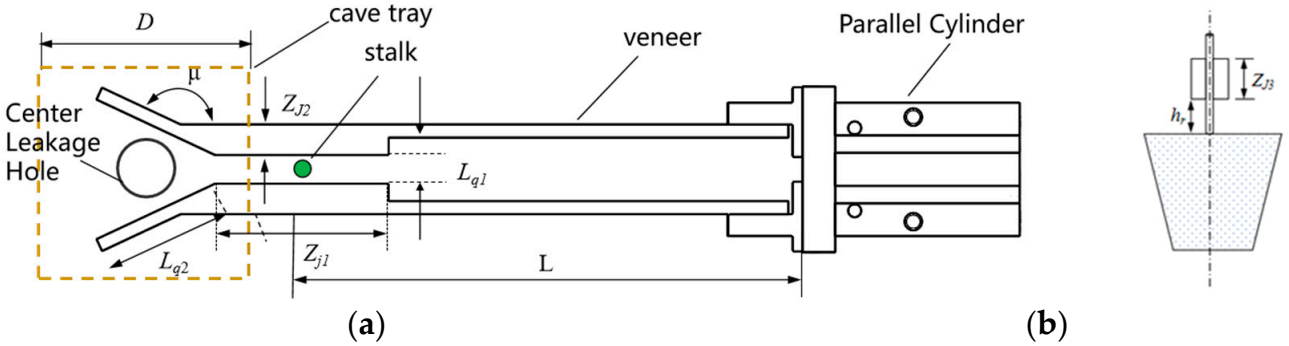


Figure 8. Structure parameter diagram of seedling clamping device. (**a**) Taking seedlings end-effector structure parameter diagram; (**b**) Side view D—the diameter of the upper opening of the hole plate. L—the length of the cantilever of the parallel cylinder clamping the stalk of the potting seedling; Z_{j1}, Z_{j2}, Z_{j3}—the length, width, and thickness of the seedling plate in the clamping position; L_{q1}—the spacing of clamping seedlings when the seedling claw is open; L_{q2}—length of the open plate; μ—opening angle of the V-shaped plate; h_r—distance between the lower part of the clamping plate and the distance between the mantle.

Based on the above three requirements, to ensure that the gripping plate can successfully grasp the seedling stems and accommodate potential deviations of the seedling tips from the center, the front end of the plate is designed as a V-shaped structure with an opening, which serves to guide and align the stems. If the length of the V-shaped plate is too long, it may damage neighboring seedlings, while if it is too short, it will fail to effectively grasp the seedlings. Therefore, the length and opening angle of the plate must satisfy the following conditions:

$$\begin{cases} L_{q1} < \sin(\pi - \mu) \times L_{q2} < \frac{D}{2} \\ \frac{D}{2} < \cos(\pi - \mu) \times L_{q2} < D \end{cases} \quad (6)$$

In the formula, L_{q1}—the spacing of clamping seedlings when the seedling claw is open, mm; L_{q2}—length of the open plate, mm; D—the diameter of the upper opening of the hole plate, mm; μ—opening angle of the V-shaped plate, °.

Based on the data analysis of the physical characteristics of the seedlings, it is found that for seedling trays aged 30–50 days, the stem diameter ranges from 2.82 to 3.44 mm. To simulate the action of manually pinching the seedling stems, 1 mm thick sponge pads are attached to both sides of the gripping plates to increase elasticity and prevent excessive pressure that may cause damage to the stems. Therefore, a closing distance of approximately 5 mm is selected to ensure proper stem gripping without the seedlings falling off. Considering the closing claw distance, the thickness of the gripping plates is set to 5 mm. To ensure successful gripping, the distances are set as follows: Z_{j1} = 20 mm, Z_{j2} = 5 mm, and Z_{j3} = 8 mm, resulting in a gripping distance L_{q1} of 10.9 mm. Using a 72-cell standard seedling tray, the upper length D of each cell is 40 mm. During the clamping process, the angle of the V-shaped plate must not interfere with adjacent trays. By substituting the data into Equation (6), the optimized parameters were obtained, with μ = 150° and L_{q2} = 30 mm.

Mechanical Analysis of the Stem Clamping Process

To ensure the smooth execution of the gripping process, a detailed mechanical analysis of the stem gripping phase was conducted. During the entire seedling extraction process, after the topping action is completed, the adhesive force and friction between the seedling tray and the tray wall gradually diminish until a stable state is reached. At this point, when lifting the seedling in the gripping state, only the seedling's own weight needs to be overcome [23]. To minimize damage to the stem, the force conditions during the gripping process were studied, leading to the selection of an appropriate gripping cylinder and a rational design of the gap between the gripping plates. As shown in Figure 9, by establishing a force equilibrium equation, we determined the magnitude and direction of the force required to lift the seedling in the gripping state.

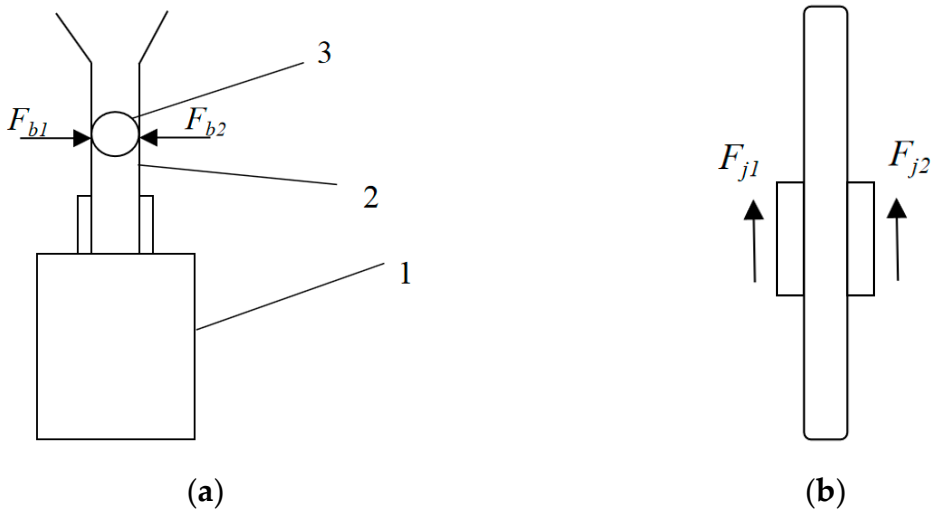


Figure 9. Analysis of the force process of stem clamping and seedling extraction. (**a**) Top view; (**b**) Side view. 1. Seedling clamping cylinder; 2. Seedling clamping plate; 3. Potting stem.

In regular operation, after grasping the stalks, the stems are elevated by the cylinder, causing them to detach from the seedling tray. According to D'Alembert's principle, one must account for the fictitious inertial forces acting on the seedlings at that moment. As a result, the seedlings exhibit a certain instantaneous upward acceleration, denoted as am, which can be derived from the equation relating displacement and acceleration.

$$x_m = v_m t_m + \frac{1}{2} a_m {t_m}^2 \tag{7}$$

In the formula, x_m—for the lift cylinder stroke, m; v_m—the initial speed, m/s; t_m—upward lifting time, s; a_m—instantaneous acceleration when taking out, m/s^2.

When working with clamping cylinders, a safety factor S is often added to prevent the work piece from falling to ensure smooth clamping. The force balance has

$$\begin{cases} F_{b1} = F_{b2} \\ F_{b1} + F_{b2} = F_b \\ F_{j1} + F_{j2} - Smg = ma_m \\ F_{j1} + F_{j2} \leqslant f_1 F_b \end{cases} \tag{8}$$

In the formula, f_1—friction coefficient between seedling claw and stem; S—safety coefficient, generally taken as 4; F_b—clamping force on both sides of the seedling claw, N; m—mass of the potting seedling, g.

Organizing is available, as follows:

$$F_b \geqslant \frac{Smg + ma_m}{f_1} \tag{9}$$

Balance equations based on moment balance, as follows:

$$F_b L = Fl_c \tag{10}$$

In the formula, l_c—parallel clamping cylinder body and the center of the force distance; F—cylinder clamping force.

We select the cylinder model TN20 × 100 s for this purpose, with a travel distance x_m of 100 mm. Given that the seedlings are smoothly removed from the tray with an initial velocity v_m of 0 and the lifting time t_m is 1 s, by substituting the data into Equation (7), we calculate the instantaneous upward acceleration to be a_m = 0.8 m/s^2. In the case of proper topping, resulting in complete separation of the seedling pot from the tray without resistance, the clamping force only needs to overcome the weight of the seedling. The friction coefficient (f_1) between the clamping plate and the seedling is taken as 0.5. By employing Equation (8), the minimum theoretical clamping force required for the clamping plate is 1.02 N. In the case of a failed seedling lifting, the separation force must also be considered. Previous experiments indicate that the separation force is 5.22 N, so the clamping force of the clamping plate F_b must be greater than 6.24 N. According to Section 2.1.2, the seedling stalk clamping force should not exceed 24.06 N, so the clamping force F_b of the clamping plate ranges from 6.24 N to 24.06 N.

Given the arrangement of the components, the design must strike a delicate harmony between preventing any interferences and ensuring successful grasping. The cantilevered length of the clamping plate, denoted as L, is 100 mm, and the lateral clearance, l_c, is 15 mm. Upon applying Formula (10), the gripping force exerted by the parallel pneumatic cylinders (F) is calculated to be 43 N under normal operating conditions of 0.5 M Pa pressure. A review of the cylinder's clamping force in relation to its swing length reveals that for the selected Jia xin pneumatic finger cylinder model MHZ2-16D, which operates in the mode of internal diameter gripping, the clamping force reaches 45 N. The closed jaw spacing, or the distance between the claws at minimum extension, measures 14.9 mm, and the maximum jaw spacing, or the opening of the jaws, is 20.9 mm, with the actuating stroke covering a range of 6 mm.

During the seedling transplanting process, deviations in the alignment of the seedling stem from the center of the tray may occur, leading to stem bending during seedling extraction. To prevent bending damage, two aspects must be addressed: first, optimizing the structure of the gripping end effector to avoid damage, and second, setting an appropriate gripping height to minimize bending-related injury. This study analyzes the stem of the chili seedling, which can be modeled as a uniform slender beam with one end fixed and the other free (ignoring its own weight, as shown in Figure 10). The focus is on determining how to set the gripping height precisely, based on the mechanical properties of stem bending, to ensure minimal damage during the gripping process. The coordinate system is established with the center of the tray as the origin O, the axial direction of the stem as the x-axis, and the radial direction as the y-axis. Point P_1 represents the fixed end of the seedling stem on the tray, and point P_2 denotes the gripping position. h_r is the bending length of the stem (gripping height).

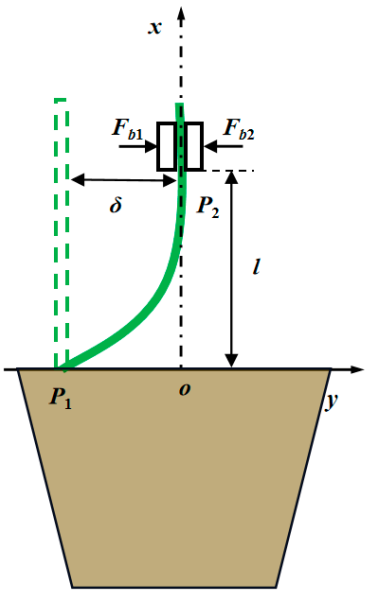


Figure 10. Schematic diagram of stem bending deformation.

Under the action of clamping force, the stalk is in an unstable state, when the approximate equation of the deflection curve is

$$y_{(x)} = \delta\left(1 - \cos\frac{\pi x}{2l}\right) \tag{11}$$

In the formula, $y_{(x)}$—stem deflection; l—stem length; δ—horizontal displacement at the stem tip; x—section position.

The bending strain energy of the stem under the clamping force is as follows:

$$U = \frac{EI}{2}\int_0^l \left(\frac{\mathrm{d}^2 y}{\mathrm{d}x^2}\right)^2 dx = \frac{EI}{2}\left(\frac{\delta\pi^2}{4l^2}\right)^2 \int_0^l \left(\cos\frac{\pi x}{2l}\right)^2 dx = \frac{EI\pi^4\delta^2}{64l^3} \tag{12}$$

At this point, the external potential energy is calculated by replacing the inertial force with an equivalent load F_c, whose potential energy is

$$V = F_c \cdot \delta \quad (x = l) \tag{13}$$

The total potential energy is then

$$\Pi = U - V = \frac{EI\pi^4\delta^2}{64l^3} - F_c\delta \tag{14}$$

By the principle of least potential energy ($\delta\Pi = 0$), the following is established:

$$\frac{\partial\Pi}{\partial\delta} = \frac{EI\pi^4\delta}{32l^3} - F_c = 0 \tag{15}$$

The bending stress of the stem at point P_1 under the critical load F_c is

$$\begin{cases} \sigma_{P1} = \frac{M_{P1}}{W_{P1}} \\ W_{P1} = \frac{I}{y} \\ I = \frac{\pi d_x^4}{64} \end{cases} \tag{16}$$

One can deduce that

$$\sigma_{P1} = \frac{64F_cL}{\pi {d_x}^4} \cdot \frac{d_x}{2} = \frac{32F_cl}{\pi {d_x}^3} \tag{17}$$

$$\delta = \frac{64l^2\sigma_{P1}}{Ed_x\pi^4} \; or \; l = \sqrt{\frac{Ed_x\pi^4\delta}{64\sigma_{P1}}} \tag{18}$$

In the formula, d_x—diameter of the stalk; E—modulus of elasticity of the stalk; W_{P1}—coefficient of bending cross-section; I—moment of inertia of the cross-section; y—centrifugal distance of the stalk; σ_{P1}—bending stress of the cross-section at the lower end point P_1.

In the case of the same bending stress at point P_1, the distance between the stalk and the centerline offset is directly associated with the clamping height of the seedling, and the two show a positive relationship, in order to prevent damage to the stalk due to excessive bending force, to ensure that the minimum clamping height h_r is satisfied, as follows:

$$h_r \geqslant l \tag{19}$$

The trials conducted by scholars like [24] have shown that tray seedlings exhibit high bending resistance, with an elasticity modulus of 34.92 MPa and a maximum bending stress of 2.52 MPa. By utilizing this information along with the test parameters (d_x = 3.21 mm, δ = 2.1 mm), upon applying the calculations in Formula (18), the curvature length l is determined to be 11.9 mm. From Section 2.1.1, it can be inferred that by compression tests, the lower stem portion demonstrates strong compressive strength. When it comes to clamping the stem, positioning is crucial; the ideal point would be about 10–20 mm below the tray, typically selecting the base of the stem, as locations too close to the medium might cause harm, while being too far could render the stem fragile. Therefore, the clamping height h_r is set at 15 mm to balance these factors and minimize potential damage.

3. Control and Pneumatic Systems

3.1. Pneumatic System Design

In the automated transplanting machine's seedling extraction mechanism, pneumatic components play a critical role. The pneumatic circuit layout, as shown in Figure 11, demonstrates the functionality of each cylinder: the seedling-ejecting cylinder A is responsible for pushing seedlings out of the seed tray; the lifting cylinder B raises the seedlings; the sliding table cylinder C moves the seedling tray; the seedling-distributing cylinder D disperses the seedlings above their respective planting cups; and the gripping cylinder E clamps the seedling stems. All cylinders are controlled by solenoid valves Z_i, enabling extension and retraction motions. Specifically, Airtac (Taipei, Taiwan) two-position five-way solenoid valves (model 4V210-08-DC24V) and three-position five-way solenoid valves (model 4V220-08-DC24V) are employed due to their durability and resistance to air leakage. Furthermore, to regulate the extension and retraction speeds of the cylinders, each is equipped with a throttle valve K_i, which adjusts the airflow rate to control motion speed. Considering the operational requirements of extracting an entire row of seedlings simultaneously, six gripping cylinders E are used to clamp and release seedlings in unison. Given their relatively low air consumption during operation, a single solenoid valve Z_5 is shared among these cylinders to control airflow, ensuring efficient and synchronized operation.

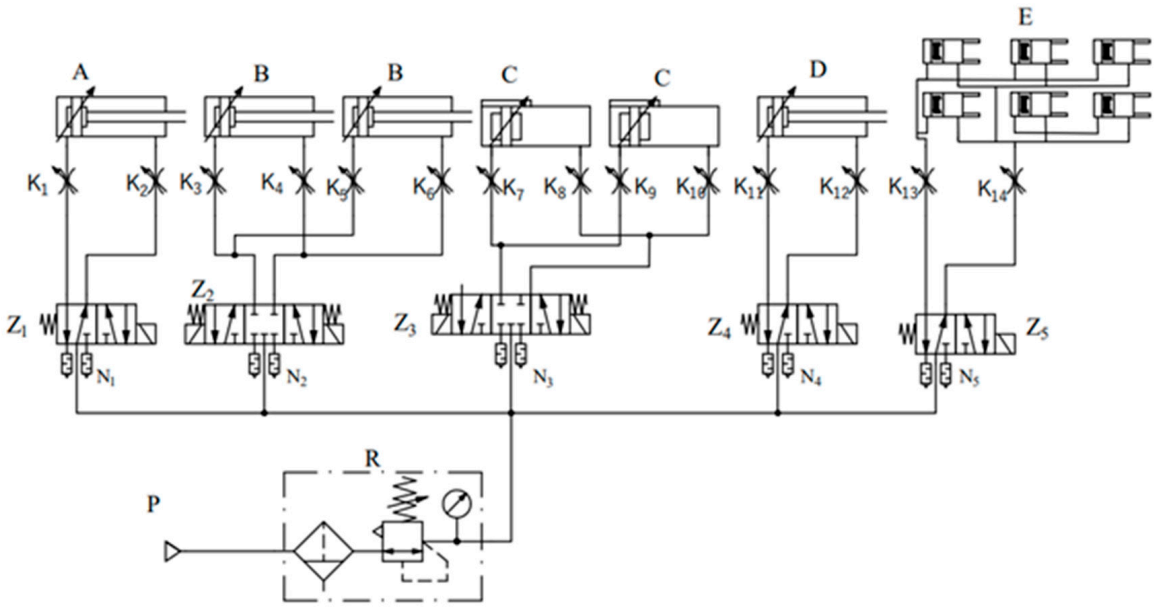


Figure 11. Pneumatic circuit schematic. P—Air source; R is the dichotomy; Z_i—Control solenoid valve; K_i—Throttle valve; N_i is the muffler; A—Seedling-ejecting cylinder; B—Lifting cylinder; C—Sliding table cylinder; D—Seedling-distributing cylinder; E—Gripping cylinder.

Calculation of Air Consumption in Pneumatic Systems

To ensure smooth operation of the pneumatic circuit, it is crucial to holistically assess the parameters indicated for the cylinder and conduct meticulous calculations to determine the precise total air demand. The influence of the picking frequency on this consumption is significant, as a higher frequency generally leads to a progressive increase in demand. Consequently, when selecting a compressor model, not only should the total air consumption be a focus but the operational frequency's impact on system performance must be thoroughly evaluated. Adequate airflow is vital for the efficient and stable functioning of the pneumatic loop, ultimately boosting the overall system efficiency. The formula for calculating the cylinder's air consumption is

$$Q = \frac{\pi}{2} N D_q^2 L_q \frac{P + 0.1}{0.1} \times 10^{-3} \tag{20}$$

In the formula, Q—cylinder air consumption; N—cylinder movement frequency; D_q—cylinder bore; L_q—cylinder stroke; P—the working pressure of the pneumatic system.

Based on the analysis above, the models for the seedling-distributing cylinder, lifting cylinder, and clamping cylinder have been determined. Additionally, through preliminary experimental analysis, the required ejection force is at least 5.22 N. The SMC thin-profile cylinder (Tokyo, Japan), model CDQSB16-30DM, with an ejection force of 25.12 N and a stroke of 30 mm, is selected as the ejection cylinder. According to the layout dimensions of the prototype, the sliding platform displacement cylinder is chosen to be the SMC mechanically actuated rodless cylinder, model MY1B25G-400, with a bore diameter of 25 mm and a stroke of 400 mm. Based on these specifications, the system's air consumption is calculated, as shown in Table 2.

Table 2. Calculation of gas consumption.

Cylinder Type	Model Number	Frequency (Times/min)	Cylinder Diameter D_q/(mm)	Stroke L_q/(mm)	Quantity	Gas Consumption Q (L/min)
Top Cylinder	CDQSB16-30DM	15	16	30	1	1.09
Lift Cylinder	TN20 × 100 s	15	20	100	2	11.31
Slide shift cylinders	MY1B25G-400	15	25	400	2	70.70
Split Cylinder	MAL20-450	15	20	450	1	25.45
Clamp cylinder	MHZ2-16D	15	16	6	6	1.30
Total						109.85

As can be seen from Table 2, in the case of a seedling picking frequency of 90 plants/min, the air consumption of the automatic transplanting machine seedling picking mechanism is 109.85 L/min; in order to ensure that the air source is sufficient and stable, we should choose the air compressor with a capacity of 120 L/min or more as the air output power source.

3.2. Control System Design

3.2.1. Programmatic Design

The core of the control system lies in its two main components: the positioning program and the seedling picking and placing program. Upon system startup, once the power is supplied, a simple press of the start button will activate the stepper motor, initiating the conveyor task. The motor will continue running until it precisely reaches the preset position. At this point, the sensor detects the signal, triggering the PLC contact to stop the motor, thus ensuring precise positioning. As the core process, the picking and placing program will ensure that after positioning, the seedling picking, spacing, and placing operations are carried out in the predefined sequence, ensuring smooth system operation. The system flow diagram (Figure 12) clearly illustrates this series of precise and orderly steps.

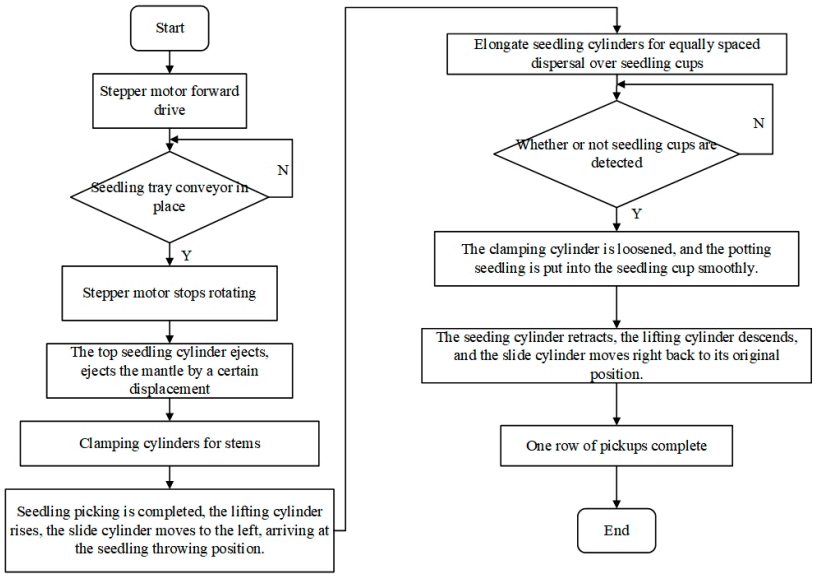


Figure 12. Flowchart of the seedling extraction control system.

3.2.2. PLC Control System Lines

Based on the working principle of the seedling picking system and by utilizing a touch screen as the upper-level controller to control the PLC system, which in turn manages the entire seedling picking and placing process, the selected touch screen model is the

TPC7032kt embedded touch screen from Kunlun Tongtai Company. This touch screen features a 7-inch LCD display and a four-wire resistive touch screen and is powered by a low-energy CPU, forming an integrated embedded touch panel. It is equipped with both RS232 and RS485 communication ports for direct communication with the Mitsubishi PLC. The editable controller model is the Mitsubishi FX_{2N}-48MT, which is user-friendly, easy to operate, and highly durable. The input signals come from the start button, pause button, emergency stop button, and photoelectric sensors, while the output signals drive various solenoid valves and stepper motor controllers for execution. The system employs motor rotation for material handling, while the seedling picking, spacing, and placing actions are carried out pneumatically. The wiring principle is shown in Figure 13, where the hardware connection layout is planned. Since different components in the seedling picking system require different voltage levels, the control system uses both 48 V and 24 V DC power supplies. The actual wiring follows this schematic, visually implementing the overall design, as shown in Figure 14.

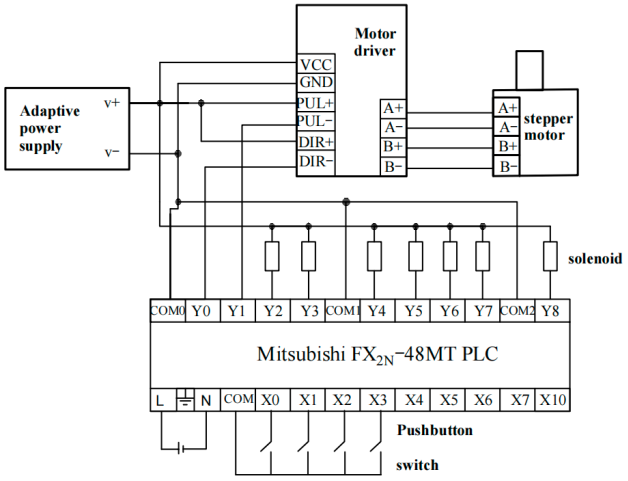


Figure 13. Circuit diagram of pick and place seedling control.

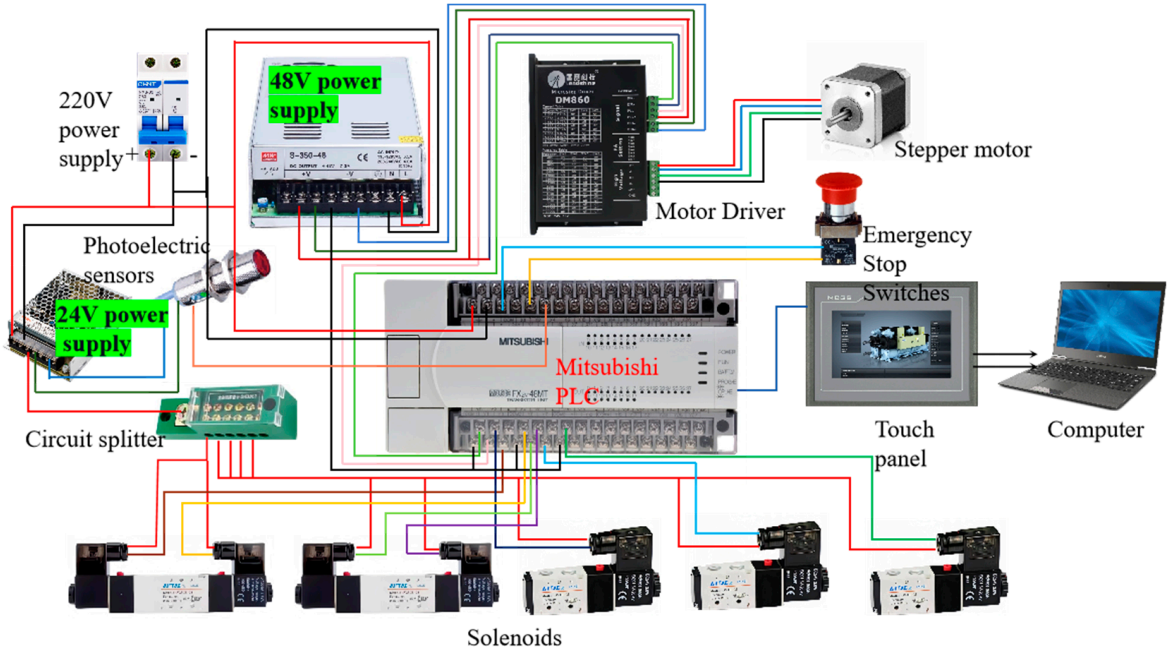


Figure 14. Physical wiring diagram.

3.2.3. Software Design

The input and output addresses of the Mitsubishi PLC controller are assigned as shown in Table 3. After importing the pre-programmed program into the PLC, the internal system controls each component to operate sequentially. The air compressor provides the power source for the cylinders, while the solenoid valves control the inflow and outflow of air, thereby regulating the movement of the cylinders.

Table 3. I/O port definitions.

Input Point	Description of Controls	Output Point	Description of Controls
M0	activation button	Y0	Direction of motor rotation
M1	Pause button	Y1	Motor pulses
X2	emergency stop button	Y2	Cylinder extension of top seedling
X3	Photoelectric sensors	Y3	Lift Cylinder Rise
		Y4	Lift Cylinder Lowering
		Y5	Shift cylinder left
		Y6	Shift cylinder right
		Y7	Seedling cylinder elongation
		Y10	Cylinder clamping

In the Mitsubishi GX-Works2 programming environment, a precise control program was assembled, utilizing a clear hierarchy of sequential control instructions and timers. As depicted in Figure 15, the output Y1 corresponds to a pulse signal input for a step motor, facilitating its control and movement in the program. Following the program development, a preliminary run test was conducted, which involved executing the code without physically connecting any elements to verify the program's smooth functionality. After confirming the test run without issues, a subsequent system debugging phase took place on an empty load prototype machine. This step aimed to ensure that all operation commands were responsive and produced the intended results. By iterating through this process, the programmer fine-tuned the program to meet the intended control performance in the actual implementation [25].

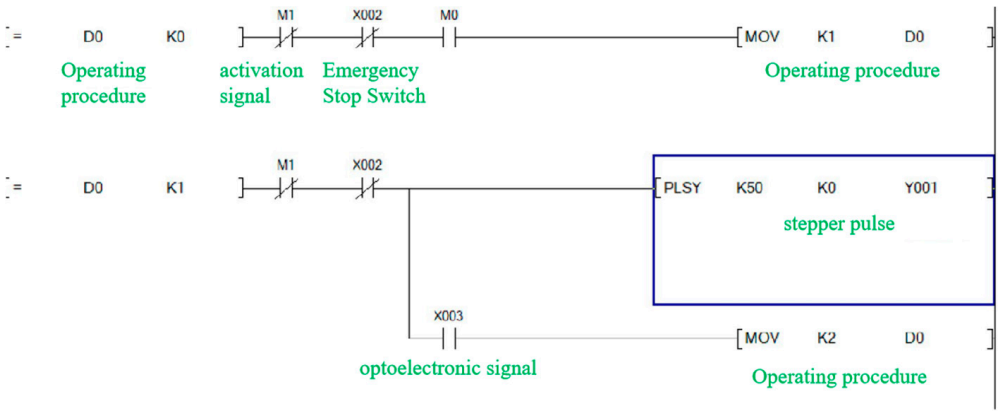


Figure 15. PLC part of the program.

4. Test Stand Experiment

4.1. Test Conditions

From 10 to 20 October 2024, performance tests for the transplanting system were conducted at the Key Laboratory of Mechanical and Automotive Engineering, Qingdao University of Technology. The prototype setup is shown in Figure 16. The test seedlings were pepper plug tray seedlings cultivated by Shandong S.G Agricultural Co., Ltd in China. The soil

substrate was a nutrient-rich mixture of vermiculite, perlite, and peat moss in a 1:1:2 ratio, which provided optimal growing conditions. The seedlings exhibited robust root systems and vigorous foliage, meeting the experimental requirements.

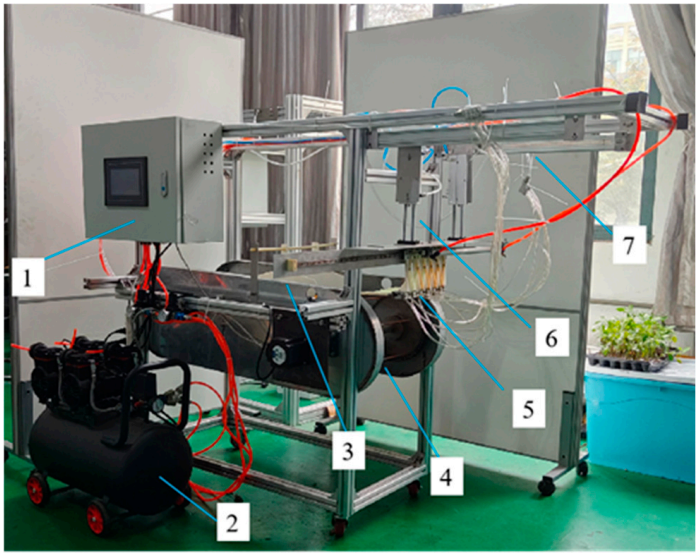


Figure 16. Test rig table. 1. Control cabinet; 2. Air compressor; 3. Platen mechanism; 4. Seedling tray conveying mechanism; 5. Seedling dividing mechanism; 6. Lifting mechanism; 7. Shifting mechanism.

The testing equipment included the Z.H ACS electronic scale and X.M precision soil moisture meter for the accurate measurement of the process parameters.

4.2. Experimental Design

Seedling age is a key determinant of stem thickness and the firmness of the plug, directly influencing transplant survival and tolerance, and thereby affecting damage rates. At 30 days of age, pepper seedlings exhibit moderate plug strength and a relatively low overlap between stems and leaves. At 40 days, the root system is more developed, and the stems and leaves become denser, increasing the likelihood of seedling damage. Therefore, seedlings aged 30, 35, and 40 days were selected for this study. The moisture content is closely related to the looseness of the plug and influences substrate loss. Proper moisture control ensures smooth seedling extraction and minimizes substrate loss. When the moisture content is too low (<30%), the substrate tends to become loose and dehydrated; when it is too high (>60%), the plug's compressive strength is reduced, leading to increased damage. Hence, the average moisture content of the substrate was set at 30%, 45%, and 60%. Seedling extraction frequency must balance the delivery of the seedling tray with the extraction rhythm. Both excessively high and low frequencies can negatively impact efficiency and success rates. A frequency that is too high may result in extraction failure, while too low a frequency can reduce extraction efficiency and fail to meet the performance requirements of high-efficiency transplanting machines. Therefore, extraction frequencies of 60, 72, and 84 seedlings per minute were chosen.

This study aims to explore the critical role of seedling age, moisture control, and optimal extraction frequency in improving extraction efficiency. These three parameters were selected as experimental factors for a three-factor three-level orthogonal experiment, with factor levels as shown in Table 4.

Table 4. Table of factor levels.

Level	Test Factor		
	Water Content A/(%)	**Seedling Age B/(d)**	**Seedling Extraction Frequency C/(Plant/min)**
−1	30	30	60
0	45	35	72
1	60	40	84

4.3. Test Methods and Evaluation Indicators

In line with the technical specifications detailed in the industry standard [JB/T10291—2013 for arid land planting machiner], modifications were made to the seedling retrieval control system catering to varying retrieval rates. The air compressor was adjusted to an operating pressure of 0.5 MPa, and a uniform watering was performed on the seedlings before measurements were taken using a moisture meter. The trials were conducted at predetermined water levels of 30%, 45%, and 60%. Reference to Section 3.2.2 determined the testing point to be at a seedling retention height of 15 mm. The evaluation was based on three critical performance metrics: seedling extraction success rate (Y_1), substrate loss rate (Y_2), and the pot seedling damage rate (Y_3). This methodological approach ensures consistency across trials while examining the respective effects on the machine's efficiency under each designated condition.

(1) Seeding Success Rate Y_1: A complete removal of seedlings from the seedling trays to the corresponding seedling cups without any damage. If the seedlings remain intact throughout the process, the retrieval is considered a success. Mathematically, it can be represented by the following formula:

$$Y_1 = \frac{S_1}{S} \times 100\% \tag{21}$$

In the formula, S_1—number of successful plants taken; S—total number of potting seedlings.

(2) Substrate Loss Rate (Y_2): In the seedling retrieval process, during both emergence and grasping, substrate chunks may break due to impact. The rate of substrate loss is evaluated by comparing the mass of the substrate before and after it is extracted from the seedling tray to fall into the seedling cup. The computation formula is as follows:

$$Y_2 = \frac{M_1 - M_2 - M_0}{M_1 - M_0} \times 100\% \tag{22}$$

In the formula, M_0—mass of seedling trays; M_1—total mass of seedlings in hole trays before the test; M_2—total mass of seedlings in pots after taking seedlings.

(3) Pot Seedling Damage Rate (Y_3): During the seedling retrieval process, seedlings' leaves and stems can sustain some level of damage. The pot seedling damage rate is calculated by comparing the number of damaged seedlings to the total number of intact seedlings after the retrieval. The formula is as follows:

$$Y_3 = \frac{S_2}{S} \times 100\% \tag{23}$$

In the formula, S_2—the number of potting seedlings stalk pinching and leaf damage plants.

5. Test Results and Discussion

5.1. Response Surface Analysis

Using Design-Expert 13.0 software, a three-factor three-level orthogonal experiment was designed, consisting of 17 experimental runs. The Box–Behnken response surface methodology was employed to determine the optimal parameter combination. The Box–Behnken design is a synthesis of statistical design and experimental techniques; we utilized Box–Behnken experimental design and obtained certain data through experiments. The Box–Behnken design uses a multivariate quadratic equation to fit the functional relationship between factors and effect values and seeks the optimal process parameters through analysis of the regression equation, which is a statistical method for solving multivariate problems.

The experimental design and results for the seedling extraction process are shown in Table 5. The specific seedling extraction process is illustrated in Figure 17.

Table 5. Seedling extraction test design and results.

Serial Number	Water Content (%)	Seedling Age (d)	Frequency of Seedling Collection (Plants/min)	Success Rate of Seedling Retrieval (%)	Substrate Loss Rate (%)	Potato Seedling Damage Rate (%)
1	45	35	72	95.24	8.59	3.57
2	30	30	72	92.67	15.8	5.95
3	30	35	60	96.67	13.65	4.17
4	30	40	72	91.67	15.28	3.57
5	60	35	60	93.06	8.65	1.39
6	30	35	84	90.48	13.87	5.56
7	60	40	72	93.06	9.86	2.38
8	45	30	60	95.83	9.6	5.56
9	60	30	72	93.06	14.63	5.95
10	60	35	84	93.33	12.68	4.44
11	45	30	84	93.25	10.84	7.78
12	45	35	72	96.43	9.68	3.57
13	45	40	84	91.67	6.85	3.33
14	45	35	72	93.16	5.87	4.44
15	45	40	60	95.83	3.37	2.78
16	45	35	72	94.44	6.68	3.57
17	45	35	72	95.24	7.52	3.57



(**a**) (**b**) (**c**)

Figure 17. Diagram of the process of picking up and dropping seedlings. (**a**). Seedling clamping process; (**b**). Splitting process; (**c**). Process of seedling dropping.

A quadratic polynomial regression model was obtained for each evaluation indicator, as follows:

$$\begin{cases} Y_1 = & 73.113 - 0.144767A + 2.3973B - 0.311708C + 0.003333AB + \\ & 0.008972AC - 0.006583BC - 0.006771A^2 - 0.03054B^2 + 0.000045C^2 \\ Y_2 = & 96.92325 - 2.14607A - 2.77005B + 0.370146C - 0.014167AB + \\ & 0.005292AC + 0.009333BC + 0.023938A^2 + 0.03354B^2 - 0.005844C^2 \\ Y_3 = & 45.57975 - 0.018783A - 2.0174B - 0.058104C - 0.003967AB + \\ & 0.002306AC - 0.006958BC - 0.000564A^2 + 0.03382B^2 + 0.001896C^2 \end{cases} \quad (24)$$

Through variance analysis of the data in Table 5, as shown in Table 6, the regression models for seedling extraction success rate Y_1, substrate loss rate Y_2, and seedling damage rate Y_3 were analyzed. The *p*-values for all models were less than 0.01, indicating that the models are significant. The *p*-values for the lack of fit terms were 0.8821, 0.7307, and 0.1429 (all greater than 0.05), indicating that the fit of the three models is good. The coefficients of determination R^2 for the fitting equations were 0.8700, 0.9200, and 0.9464 (all greater than 0.8), suggesting that over 87% of the response values can be explained by these three models. Therefore, these models can be used to predict the operating parameters of the automated seedling extraction device.

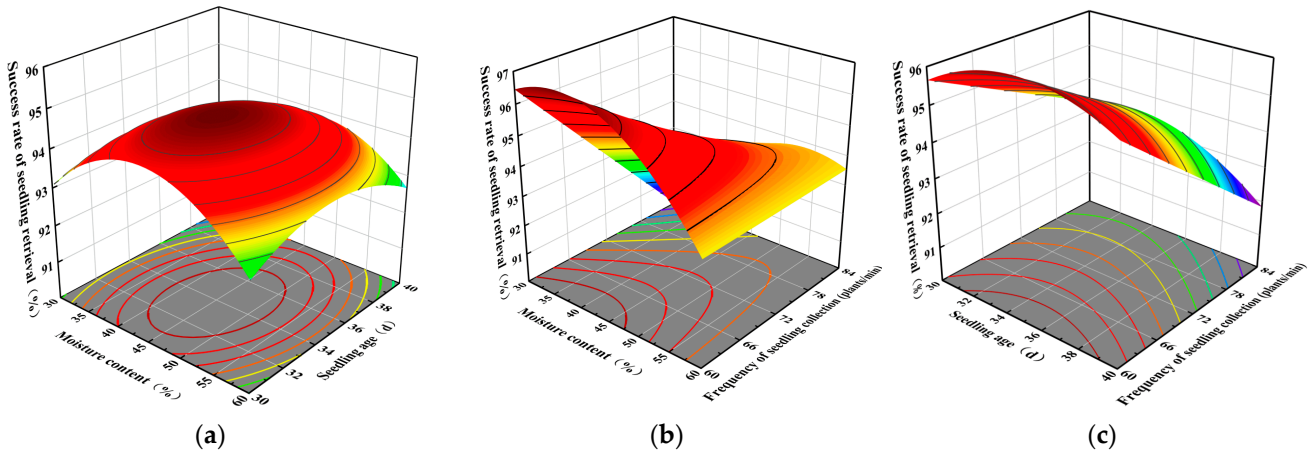
Table 6. Results of analysis of variance for each indicator.

Evaluation Indicators	Source	Sum of Squares	F	*p*
Success rate of seedling retrieval	model	45.14	5.21	0.0204
	A	0.1301	0.135	0.7242
	B	0.832	0.8637	0.3836
	C	20.03	20.8	0.0026
	lost proposal	0.9326	0.214	0.8821
	R^2		0.8700	
Substrate loss rate	model	198.44	12.64	0.0015
	A	20.42	11.7	0.0111
	B	30.07	17.23	0.0043
	C	10.06	5.76	0.0474
	lost proposal	3.09	0.4507	0.7307
	R^2		0.9420	
Potato seedling damage rate	model	36.64	13.72	0.0011
	A	3.24	10.91	0.0131
	B	21.71	73.18	<0.0001
	C	6.5	21.9	0.0023
	lost proposal	1.47	3.24	0.1429
	R^2		0.9464	

Based on the experimental results, the study delved into the influence of water content (A), seedling age (B), and harvesting frequency (C) on the performance indicators. Using the Design-Expert 13.0 software, mathematical models for the pairwise interaction factors were derived. Additionally, 3D response surface plots of seedling extraction success rate (Y_1), substrate loss rate (Y_2), and seedling damage rate (Y_3) were generated using Origin 2018 software.

As shown in Figure 18a, when the extraction frequency is 72 seedlings/min, the extraction success rate initially increases and then decreases as the moisture content increases. With the increase in seedling age, the success rate first increases and then decreases, with a slight fluctuation. When both moisture content and seedling age change, the extrac-

tion success rate ranges from 92% to 94.5%, with minimal variation, indicating that the influence of these two factors on the success rate is not significant within the investigated levels. The highest peak occurs at a moisture content of 45% and a seedling age of 35 days, with a success rate reaching 96.43%. The reason for this is that excessively high moisture content leads to excessive substrate moisture, making the substrate block sticky, which causes deviation during extraction, reducing the uprightness of the seedlings. Furthermore, older seedlings lead to more developed branches and leaves within the plug tray, which can interfere with each other, thus increasing the difficulty of extraction. As shown in Figure 18b, at a seedling age of 35 days, when the extraction frequency is 60 seedlings/min, the extraction success rate increases and then decreases as the moisture content increases. The decline in success rate is particularly noticeable at a moisture content of 30%, and this phenomenon becomes more pronounced as the frequency increases. In contrast, when the moisture content is raised to 60%, the extraction frequency has little effect on the success rate. However, the overall success rate remains suboptimal. At the highest speed (high extraction frequency) and the lowest moisture content (low moisture content), the extraction success rate is at its lowest, at only 90.48%. The analysis suggests that the higher extraction frequency causes faster machine movement, and the low moisture content makes the substrate loose, leading to tipping of the plug tray during extraction and bending of the seedlings, thus increasing the probability of failure. As shown in Figure 18c, at a moisture content of 45%, the extraction success rate increases and then decreases with the growth of seedling age, with a smaller fluctuation. At any given seedling age, the extraction success rate generally decreases as the extraction frequency increases, with a larger amplitude. This suggests that the extraction frequency has a greater impact on the success rate than seedling age. At a seedling age of 35 days and an extraction frequency of 72 seedlings/min, the extraction success rate reaches a maximum of 96.43%. The reason for this is that with an increased extraction frequency, the movement of various components intensifies, and during the seedling gripping process, the seedlings may be lifted before they are fully grasped, leading to failure.



(**a**) (**b**) (**c**)

Figure 18. Response surface analysis of seedling extraction success. (**a**) Effect of water content and seedling age on seedling extraction success; (**b**) Effect of water content and seedling extraction frequency on seedling extraction success; (**c**) Effect of seedling age and seedling extraction frequency on seedling extraction success.

As shown in Figure 19a, at an extraction frequency of 72 seedlings/min, the substrate loss rate initially decreases and then increases as the moisture content increases, at any given seedling age. At a seedling age of 30 days, the change in substrate loss rate is more significant compared to a seedling age of 40 days, indicating that a smaller seedling age

has a more pronounced effect on substrate loss rate. At any given moisture content level, the substrate loss rate decreases as seedling age increases. However, substrate loss is higher at low moisture content compared to high moisture content. At a moisture content of 45% and a seedling age of 35 days, the substrate loss rate is at its lowest, reaching 5.87%. The reason for this is that as seedling age increases, the root system becomes more developed, and the substrate block becomes more compact, reducing substrate loss during the extraction and gripping process. As shown in Figure 19b, at a seedling age of 35 days, at any given extraction frequency, the substrate loss rate decreases and then increases as moisture content increases. At an extraction frequency of 60 seedlings/min, the variation in substrate loss rate is more noticeable. However, as the extraction frequency increases, the amplitude of the variation in substrate loss rate decreases, suggesting that moisture content has a greater impact on substrate loss rate than extraction frequency. The reason for this is that at the same seedling age, when the moisture content is too high, the substrate block softens, and when the moisture content is too low, the substrate block becomes loose, dry, and difficult to form, reducing its stickiness, which in turn affects substrate loss. At a moisture content of 45% and a lower extraction frequency, the substrate loss rate reaches its minimum, at 5.87%. As shown in Figure 19c, at a moisture content of 45%, the substrate loss rate decreases significantly as seedling age increases and increases with the increase in extraction frequency. This indicates that both seedling age and extraction frequency significantly influence the substrate loss rate. At a seedling age of 40 days and an extraction frequency of 60 seedlings/min, the substrate loss rate is minimized, reaching 3.37%. This is primarily due to the more developed root system of older seedlings, which increases the compactness of the substrate block. Additionally, a lower extraction frequency ensures better grip on the seedling plug, reducing substrate loss. Conversely, when the extraction frequency increases, the vibration of the machine intensifies, causing the substrate block to become loose at lower moisture content. The interaction between these two factors leads to a higher substrate loss rate.

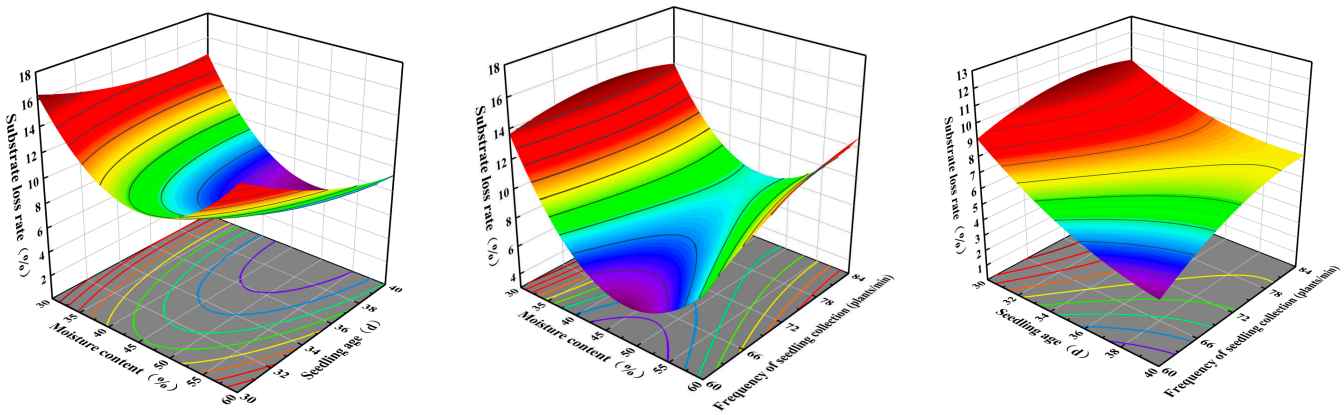
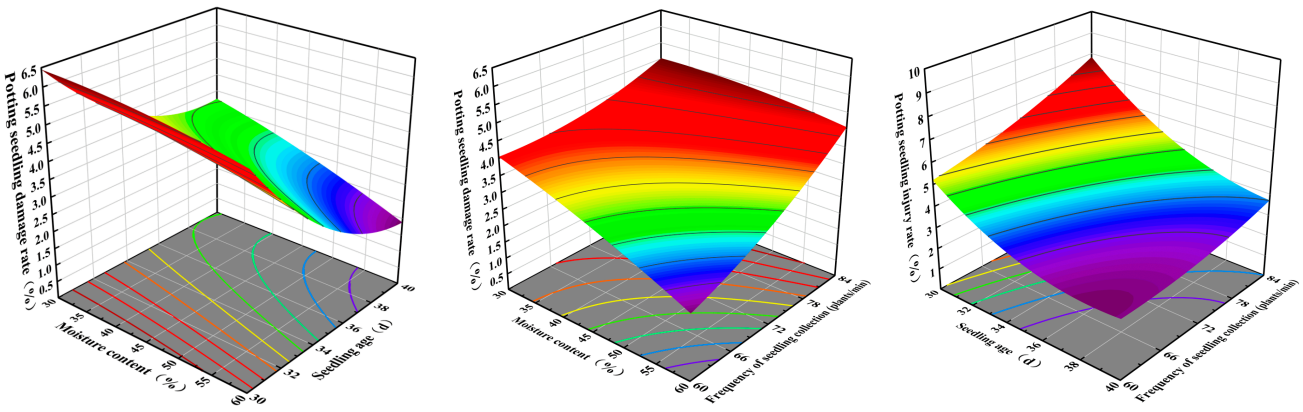


Figure 19. Substrate loss rate response surface analysis. (**a**) Effect of water content and seedling age on substrate loss rate; (**b**) Effect of water content and seedling pickup frequency on substrate loss rate; (**c**) Effect of seedling age and seedling pickup frequency on substrate loss rate.

As shown in Figure 20a, at an extraction frequency of 72 seedlings/min, the seedling damage rate decreases with the increase in seedling age at any given moisture content level, with a significant change in amplitude. When the seedling age is at its minimum, the seedling damage rate shows minimal response to varying moisture contents and is in a higher damage stage. However, at older seedling ages, the seedling damage rate decreases as moisture content increases, although the trend is more gradual, indicating

that seedling age has a more significant impact on seedling damage rate than moisture content. At a seedling age of 40 days and a moisture content of 60%, the seedling damage rate is minimized to 2.38%. This is due to the fact that older seedlings have thicker more upright stems, which makes it easier to grasp the seedling stem during extraction, thus reducing damage. As shown in Figure 20b, at a seedling age of 35 days, when the extraction frequency is low, the seedling damage rate decreases as moisture content increases, with a large variation in amplitude. When the extraction frequency exceeds 72 seedlings/min, the seedling damage rate shows no significant variation with changes in moisture content. At low moisture content, the seedling damage rate shows no significant variation with changes in extraction frequency, but at higher moisture content, the damage rate increases as extraction frequency increases. At a moisture content of 60% and an extraction frequency of 60 seedlings/min, the seedling damage rate reaches its lowest point at 1.39%. This is due to the interaction between moisture content and extraction frequency, which results in the minimum seedling damage rate. As shown in Figure 20c, at a moisture content of 45%, the seedling damage rate decreases as seedling age increases at any given extraction frequency. However, at higher extraction frequencies, the amplitude of change in the damage rate is more noticeable compared to lower extraction frequencies. At a seedling age of 30 days, the seedling damage rate increases significantly with increasing extraction frequency, while at a seedling age of 40 days, the damage rate increases slowly with higher extraction frequency. At a seedling age of 30 days and an extraction frequency of 84 seedlings/min, the seedling damage rate is highest at 7.78%. This is because the stems of younger seedlings are more fragile and tend to bend, and with the higher extraction frequency, the machine speed increases. During the gripping process, the downward motion of the end actuator may cause the seedling stem to break, leading to an increase in the seedling damage rate.



(**a**) (**b**) (**c**)

Figure 20. Response surface analysis of potting seedling damage rate. (**a**) Effect of water content and seedling age on potting seedling injury rate; (**b**) Effect of water content and pickup frequency on potting seedling injury rate; (**c**) Effect of seedling age and pickup frequency on potting seedling injury rate.

5.2. Optimization and Validation of Seedling Extraction Parameters

According to the results of the orthogonal test, water content, seedling age, and frequency of seedling extraction have a greater impact on the effect of seedling extraction; in order to obtain the highest success rate of seedling extraction Y_1, the lowest rate of

substrate loss Y_2 and the lowest rate of damage to potting seedling Y_3 are employed as the evaluation indexes, with the establishment of following mathematical models:

$$\begin{cases} \max Y_1(A,B,C) \\ \min Y_2(A,B,C) \\ \min Y_3(A,B,C) \\ s.t \begin{cases} 30\% \leqslant A \leqslant 60\% \\ 30d \leqslant B \leqslant 40d \\ 60\ Plants/\min \leqslant C \leqslant 84\ Plants/\min \end{cases} \end{cases} \tag{25}$$

The parameter optimization was performed using Design-Expert 13.0 software, yielding the following optimal combination: substrate moisture content of 47.80%, seedling age of 38.32 days, and transplanting frequency of 60 plants/min. Under these conditions, the corresponding transplanting success rate was 95.90%, substrate loss rate was 3.99%, and seedling damage rate was 2.44%. Given the difficulty of precisely adjusting the substrate moisture content of the seedling trays to the theoretical values in practical trials, parameters close to the theoretical values were selected for the verification experiment. The chosen parameter combination for verification was substrate moisture content of 48%, seedling age of 38 days, and transplanting frequency of 60 plants/min.

In the verification experiment, the same 72-cell chili seedling trays used in the study were tested on the identical experimental setup. To ensure accuracy, the environmental conditions were kept consistent with those in the initial experimental phase. The verification trials were repeated three times, with data recorded after each trial and the average values calculated. The final results showed a transplanting success rate of 94.44%, a substrate loss rate of 6.07%, and a seedling damage rate of 4.17%. The actual results exhibited minimal deviation from the optimized predictions, demonstrating stable device performance and confirming that the optimized operational parameters are reliable and applicable for practical use.

The automatic seedling extraction device designed in this study, which combines the top-loosening and stem-clamping method, achieves a seedling extraction success rate of 94.44%, substrate loss rate of 6.07%, and seedling damage rate of 4.17%. Compared to traditional seedling extraction devices, it demonstrates stable performance, higher working efficiency, and a significantly improved seedling extraction success rate (94.44%). Compared to clamping-type extraction devices (where seedling damage rates typically range from 5–10%), our method eliminates the damage caused by stem strength, with the seedling damage rate controlled at 4.17%. In comparison to top-pushing extraction devices, our method greatly reduces the impact of pot strength and the adhesion between the tray and the pot, leading to a reduced substrate loss rate of 6.07%, thereby lowering the production costs.

6. Conclusions

This study presents a fully automated row-based seedling extraction mechanism based on mechanical principles and pneumatic control design. The system consists of a frame, seedling tray conveying device, seedling extraction device, pneumatic system, and control system, among others. Key working components have been optimized to enable automatic operations such as seedling delivery, extraction, clamping, and distribution. The design is simple and easy to control.

Using a 72-cell pepper seedling tray as the research subject, mechanical characteristic tests of seedling stems were conducted. Based on the results, a force model during the clamping process was established, leading to the optimization of the clamping mechanism. Furthermore, a kinematic model of the seedling distribution mechanism was developed to optimize the design of its key parameters. The automatic seedling extraction system's elec-

trical and pneumatic circuits were designed based on a PLC controller to ensure smooth system operation and meet design requirements.

A three-factor three-level orthogonal experiment was conducted with seedling age, moisture content, and extraction frequency as experimental factors and seedling extraction success rate, substrate loss rate, and seedling damage rate as evaluation indicators. Variance analysis and response surface analysis were used to determine the influence of key factors on these indicators. Using Design-expert 13.0 software, the optimization parameters were solved, resulting in the optimal conditions for the highest seedling extraction success rate, lowest substrate loss rate, and minimum seedling damage rate when the seedling moisture content is 48%, the seedling age is 38 days, and the extraction frequency is 60 seedlings/min. A verification test using the same parameters confirmed that under the optimal parameter combination, the seedling extraction success rate was 94.44%, the substrate loss rate was 6.07%, and the seedling damage rate was 4.17%, all of which meet the design requirements.

In contrast to traditional agricultural machinery, this study integrates machine-electro-pneumatic automation, combining advanced technologies such as sensor positioning and programmable control. The system includes numerous moving parts, which require high installation precision and compatibility. During testing, issues such as insufficient sealing between some components and machine vibration were observed. Future improvements will focus on optimizing the overall structural dimensions and reducing the number of pneumatic components to prevent air leakage. The program will continue to be updated and optimized to simplify the movement process, increase the seedling extraction frequency, and achieve accurate and rapid seedling placement. The system will gradually evolve toward intelligence and visualization.

Author Contributions: Writing—original draft preparation, Z.P.; writing—review and editing, F.Y.; supervision, X.L.; the collection and organization of experimental data, Y.L.; investigation, B.L. and G.X. All authors have read and agreed to the published version of the manuscript.

Funding: This research was funded by the National Natural Science Foundation of China, Grant number 52202508, and the Science and Technology Planning Project of Xinjiang Production and Construction Corps, grant number 2024AB047.

Institutional Review Board Statement: Not applicable.

Data Availability Statement: The data presented in this study are available on request from the corresponding author.

Acknowledgments: The authors are grateful to anonymous reviewers for their comments.

Conflicts of Interest: The authors declare no conflicts of interest.

References

1. Liu, W.; Tian, S.J.; Wang, Q.Y.; Jiang, H.Y. Key Technologies of Plug Tray Seedling Transplanters in Protected Agriculture: A Review. *J. Agric.* **2023**, *13*, 1488. [CrossRef]
2. Cheng, B.; Wu, H.; Zhu, H.; Liang, J.; Miao, Y.; Cui, Y.; Song, W. Current Status and Analysis of Key Technologies in Automatic Transplanters for Vegetables in China. *Agriculture* **2024**, *14*, 2168. [CrossRef]
3. Liao, Q.X.; Zhang, Z.; Hu, Q.L. Design and trajectory analysis of pneumatic picking-up mechanism for rape paper pot seedling. *Trans. Chin. Soc. Agric. Mach.* **2017**, *48*, 70–78.
4. Ye, B.; Zeng, G.J.; Deng, B.; Yang, C.L.; Liu, J.K.; Yu, G.H. Design and tests of a rotary plug seedling pick-up mechanism for vegetable automatic transplanter. *J. Int. J. Agric. Biol. Eng.* **2020**, *13*, 70–78. [CrossRef]
5. Sharma, A.; Khar, S. Current developments in vegetable transplanters in developing countries: A comprehensive review. *Int. J. Veg. Sci.* **2022**, *28*, 417–440. [CrossRef]
6. Jin, X.; Zhang, B.; Suo, H.; Lin, C.; Ji, J.; Xie, X. Design and Mechanical Analysis of a Cam-Linked Planetary Gear System Seedling Picking Mechanism. *Agriculture* **2023**, *13*, 810. [CrossRef]

7. Li, P.; Yun, Z.; Gao, K.; Si, L.; Du, X. Design and Test of a Force Feedback Seedling Pick-Up Gripper for an Automatic Transplanter. *Agriculture* **2022**, *12*, 1889. [CrossRef]
8. Abhijit, K.; Mathur, S.M.; Gaikwad, B.B. Automation in Transplanting: A Smart Way of Vegetable Cultivation. *J. Curr. Sci.* **2018**, *115*, 1884–1892. [CrossRef]
9. Islam, M.N.; Iqbal, M.Z.; Chowdhury, M.; Ali, M.; Shafik, K.; Kabir, M.S.N.; Lee, D.-H.; Chung, S.-O. Stress and Fatigue Analysis of Picking Device Gears for a 2.6 kW Automatic Pepper Transplanter. *Appl. Sci.* **2021**, *11*, 2241. [CrossRef]
10. Ma, G.X.; Chen, X.; Liu, Y.; Han, L.H.; Mao, H.P.; Hu, J.P. Airflow ejection-wrapped clamping type seedling picking method and parameter optimization. *J. Front. Plant Sci.* **2023**, *13*, 1084563. [CrossRef]
11. Jiang, L.; Zhu, T.W.; Tang, Q.; Wu, J.; Jiang, D.; Huang, M.H. Mechanical Characteristics Testing and Parameter Optimization of Rapeseed Blanket Seedling Conveying for Transplanters. *Agriculture* **2024**, *14*, 699. [CrossRef]
12. Islam, M.N.; Iqbal, M.Z.; Ali, M.; Chowdhury, M.; Kabir, M.S.N.; Park, T.; Kim, Y.-J.; Chung, S.-O. Kinematic Analysis of a Clamp-Type Picking Device for an Automatic Pepper Transplanter. *Agriculture* **2020**, *10*, 627. [CrossRef]
13. Yang, Q.Z.; Xu, L.; Shi, X.Y.; Ibrar, A.; Mao, H.P.; Hu, J.P.; Han, L.H. Design of seedlings separation device with reciprocating movement seedling cups and its controlling system of the full-automatic plug seedling transplanter. *J. Comput. Electon. Agric.* **2018**, *147*, 131–145. [CrossRef]
14. Yue, R.; Hu, J.P.; Liu, Y.J.; Yao, M.J.; Zhang, T.F.; Shi, J.W. Design and Working Parameter Optimization of Pneumatic Reciprocating Seedling-Picking Device of Automatic Transplanter. *Agriculture* **2022**, *12*, 1989. [CrossRef]
15. Jin, X.; Zhao, K.X.; Ji, J.T.; Ma, H.; Pang, J.; Qiu, Z.M. Design and experiment of automatic transplanting device for potted tomato seedlings. *J. Proc. Inst. Mech. Eng. Part C J. Mech. Eng. Sci.* **2019**, *233*, 1045–1054. [CrossRef]
16. Khadatkar, A.; Magar, A.P.; Sawant, C.P.; Modi, R.U. Development and testing of automatic seedling extractor in robotic transplanter using mechatronics for nursery seedlings. *Discov. Appl. Sci.* **2024**, *6*, 51. [CrossRef]
17. Liu, Z.C.; Shi, L.; Liu, Z.Y.; Xing, J.F.; Hu, C.; Wang, X.F.; Wang, L. Design and Testing of a Seedling Pick-Up Device for a Facility Tomato Automatic Transplanting Machine. *Sensors* **2024**, *24*, 6700. [CrossRef]
18. Zhou, M.L.; Sun, H.; Xu, X.; Yang, J.J.; Wang, G.B.; Wei, Z.X.; Xu, T.B.; Yin, J.J. Study on the Method and Mechanism of Seedling Picking for Pepper (*Capsicum annuum* L.) Plug Seedlings. *Agriculture* **2024**, *14*, 11. [CrossRef]
19. Rahul, K.; Raheman, H.; Paradkar, V. Design and development of a 5R 2DOF parallel robot arm for handling paper pot seedlings in a vegetable transplanter. *J. Comput. Electron. Agric.* **2019**, *166*, 105014. [CrossRef]
20. Zhou, B.; Miao, H.; Guan, C.S.; Ji, X.; Wang, X.C. Design and Test of Seedling-Picking Mechanism of Fully Automatic Transplanting Machine. *Appl. Sci.* **2024**, *14*, 9235. [CrossRef]
21. Hu, S.Y.; Hu, M.J.; Yan, W.; Zhang, W.Y. Design and Experiment of an Integrated Automatic Transplanting Mechanism for Picking and Planting Pepper Hole Tray Seedlings. *Agriculture* **2022**, *12*, 557. [CrossRef]
22. Wang, X.; Liu, M.Z.; Zhai, C.Y.; Han, C.J.; Yang, S.; Gao, Y.Y. Design and test of a stem clamping type seedling extraction device for vegetable transplanting. *J. Trans. Chin. Soc. Agric. Mach.* **2023**, *54*, 122–132.
23. Zhang, N. *Design and Test of Key Components of Automatic Transplanting Machine for Pepper Hole Tray Seedlings*; Huazhong Agricultural University: Wuhan, China, 2023.
24. Hu, S.Y.; Hu, M.J.; Zhang, W.Y.; Jiang, Z. Experimental and simulation studies on the mechanical characteristics of stem of chili pepper hole tray seedlings. *J. J. Chin. Agric. Mech.* **2022**, *43*, 9–18.
25. Li, M.Y.; Xiao, L.Q.; Ma, X.Q.; Yang, F.; Jin, X.; Ji, J.T. Vision-Based a Seedling Selective Planting Control System for Vegetable Transplanter. *Agriculture* **2022**, *12*, 2064. [CrossRef]

Disclaimer/Publisher's Note: The statements, opinions and data contained in all publications are solely those of the individual author(s) and contributor(s) and not of MDPI and/or the editor(s). MDPI and/or the editor(s) disclaim responsibility for any injury to people or property resulting from any ideas, methods, instructions or products referred to in the content.